Enhancing Fatigue Strength by Ultrasonic Impact Treatment

Sougata Roy* **and John W. Fisher**

ATLSS Engineering Research Center, Lehigh University, 117 ATLSS Drive, Bethlehem, PA 18015, USA

Abstract

Enhancement in fatigue performance of welded joints by Ultrasonic Impact Treatment (UIT) was evaluated in large-scale specimens having a nominal yield strength of 345 to 690 MPa. Eighteen rolled-beam specimens having welded details at cover plates and transverse stiffeners and eight built-up specimens having only transverse stiffener details were fatigue tested after treating them by UIT. A partial factorial experiment was conducted at various levels of stress range between 52 and 201 MPa, and at various levels of minimum stress, resulting in stress ratios not exceeding 0.6. Test results indicated that UIT enhanced the fatigue performance of all treated details by improving the weld toe profile, changing microstructure, and introducing beneficial compressive residual stresses at the treated region. The treatment effectively elevated the fatigue limit without changing the slope of the S-N curve in the finite life region. Fatigue design guidelines for the AASHTO Category E′ and Category C′ details were proposed and fatigue strength of a treated detail for infinite life was estimated by a simplified stress-life approach using Finite Element Analysis.

Keywords: fatigue design guideline, fatigue life enhancement, fatigue limit, post-weld treatment, ultrasonic impact treatment, welded joint

---

*Corresponding author
Tel: +1-610-758-5822; Fax:+1-610-758-5553
E-mail: sougata.roy@lehigh.edu

1. Introduction

Long term performance of welded steel structures subjected to dynamic loading has been mostly affected by development of fatigue cracks from the joints and attachments. The serviceability limit state of fatigue fracture limits effective utilization of the ultimate capacity of a structural component as design against premature fatigue cracking, according to most of the current structural codes, requires the fitness of a welded detail to be matched with imposed in-service stress levels and its endurance requirement. Since the fatigue strength of welded joints is independent of the grade of steel (Fisher et al., 1970, Fisher et al., 1974), this limitation is all the more severe in case of modern high performance steels (HPS) that are increasingly being used in bridge applications because of excellent combination of increased strength, high toughness, and improved weldability. To overcome this shortcoming it is therefore desirable to improve the fatigue resistance of common attachment details that experience crack growth from a weld toe such as, transverse stiffeners, cover plates, gusset plates, bulkheads, and other transverse welded details. In the current AASHTO Specification (2003), fatigue resistances of these as-welded details are defined by Categories C′, D, E, or E′.

Over the past decade, UIT has evolved as a promising technique for enhancement of fatigue strength of welded joints. The method involves post-weld deformation treatment of weld toe by impacts from single or multiple indenting needles excited at ultrasonic frequency, generating force impulses on the work surface (Statnikov 1997a, 1999). The objective of the treatment is to introduce beneficial compressive residual stresses at the treated weld toe, and to reduce stress concentration by improving the weld toe profile. The UIT equipment comprises: a handheld tool consisting of an ultrasonic

transducer, a wave guide, and a holder with striking needles; an electronic control box; and a water pump (Fig. 1). The tool is easy to operate and provides a comfortable working condition with minimum noise and vibration. Several choices of heads and tips are available for application to different detail types and treatment conditions. Compared to traditional "impact" treatment methods such as, air hammer peening, shot peening, and needle peening, UIT is claimed to be more efficient involving a complex effect of strain hardening, reduction in weld strain, relaxation in residual stress, reduction in operating stress concentration, and thereby achieving a deeper cold worked metal layer (Statnikov 1997a). Various investigators (Haagensen et al., 1998, Statnikov, 1997b, Trufyakov et al., 1995, Wright, 1996) reported that the fatigue performance of welded joints, albeit in small size specimens, improved by 50 - 200% at $2x10^6$ cycles, following UIT.

A pilot study conducted at Lehigh University on three large-scale welded built-up girders, made of HPS Grade 485W and having nominal yield stress (F_y) of 485 MPa, verified that fatigue performance of weld details such as, stiffeners and cover plates, could be significantly improved by application of UIT (Takamori and Fisher, 2000). These tests were conducted at stress ratio (R) of minimum stress (S_{min}) to maximum stress (S_{max}) ≤ 0.1. Only one of the treated stiffener details, an AASHTO Category C′ detail if untreated, developed a fatigue crack after achieving AASHTO Category B fatigue resistance, which is the detail category for longitudinal web-flange weld. Fatigue failure from as-welded details and flange surface defects prevented obtaining data from other treated details. Subsequently, a research project was undertaken at Lehigh University in order to define the fatigue resistance of transverse welds at stiffeners and cover plate ends treated by UIT, in full size specimens. The first part of the research program focused on

rolled beam sections, thereby eliminating the fatigue limit state at the web-flange junction. This phase of tests yielded fatigue design guidelines for treated cover plate end welds only. In a follow up phase, built-up girders fabricated from a new Cu-Ni HPS, developed at Lehigh University (Gross and Stout, 2001), were tested to establish conclusively the fatigue design guidelines for treated transverse stiffener welds. This paper describes the fatigue test program conducted on the rolled beam and the HPS girder specimens, and discusses the development of specification recommendations based on data from all the large scale tests.

2. Description of Experiments

2.1 Design Variables

Earlier studies conducted by Fisher et al. (1970 and 1974) determined that detail type and stress range (S_r) were the only two variables that significantly influenced the fatigue strength of as-welded details, although two variables S_{min} and S_r or, S_{max} and S_r or, S_{min} and S_{max} or, S_r and R or, S_r and S_m (S_m: mean stress), are needed to define the fatigue loading. A major reason behind this conclusion was the existence of localized tensile residual stresses to the order of yield stress in the weldments and in the adjoining base metal produced by shrinkage during the cooling process after welding. In the initial stages of fatigue crack growth from inherent crack-like defects in an as-welded detail, most of the fatigue life occurs in this region of high tensile residual stress. Under cyclic loading the material around the internal flaws in this area is always subjected to a fully effective tensile stress cycle even in some cases of stress reversal. S_{max} is usually at the yield point and thus S_r becomes the only stress parameter affecting fatigue strength of a detail. As a result, the effective stress ratio R is always positive and mostly greater than

0.5 in the applied range of S_r and, therefore, the second parameter does not play a significant role in the description of fatigue strength of as-welded details. However, this simplification is no longer valid when a weld toe is treated by post-weld enhancement techniques employing plastic deformation of the surface. As a result of the treatment, high tensile residual stress associated with the as-welded joint is replaced by compressive residual stresses, and the effective stress range resulting from the superposition of the applied and residual stresses can become tensile or compressive depending on their relative magnitude. As such, the fatigue strength of a treated joint becomes dependent of the second stress parameter. Previous research on improvement of fatigue resistance by post-weld treatments, that involved modification of residual stresses through plastic deformation (Booth, 1981, Fisher et al., 1979, Gurney, 1979, Maddox, 1991, Smith and Hirt., 1985), suggested that particularly at the low stress range or in the high fatigue cycle regime the treated details became unfavorably sensitive to factors that were less significant to crack growth than to crack initiation, such as S_{min} or R and the stress history. While substantial improvement could be realized at low S_{min} or R, the beneficial effect of the treatment seemed to have virtually disappeared at high S_{min}. As such, S_{min} and S_r were selected as the control stress variables for this study. In addition, for weld details improved by residual stress methods, it is anticipated that the benefits from improved joints will generally increase with yield strength due to introduction of higher beneficial compressive residual stress. Accordingly, specimens fabricated from two grades of steel having $F_y \approx$345 and 690 MPa were investigated in this program.

Transverse weld between a stiffener and the tension flange, and transverse weld at the end of a cover plate were the two details investigated. The transverse stiffener details

and connection plates in a bridge girder are defined as Category C′ in AASHTO specification (2003), whether welded to the web alone or to the web and the flange. This welded connection experiences fatigue crack growth from the toe of transverse weld, and if suppressed by post-weld treatment, the overall fatigue strength of a bridge girder could be increased to that of a welded detail developing fatigue crack from root discontinuities such as, the longitudinal web-flange weld. Fatigue strength of the longitudinal web-flange weld is defined by detail Category B, the upper bound to the AASHTO fatigue resistance curves for as-welded details. Welded cover plated beam having beam flanges greater than 19 mm is defined by detail Category E′ (AASHTO, 2003), the lower bound to the fatigue resistance curves. Although cover plate detail is rarely used in bridges these days, this detail type was selected to quantify the maximum improvement in fatigue strength that could be achieved by UIT. It was also reported in the literature that failure mode of welded details subsequent to enhancement by post-weld treatment changed to fatigue crack growth from fabrication defects at the weld root. For optimum performance of toe treatment, it is therefore desirable to match the fatigue crack growth life from root defects to the fatigue life of the treated toe. Previous studies (Gurney, 1979, Takamori, 1999) demonstrated that larger size fillet weld reduced stress concentration adjacent to the weld root, contributing to increased fatigue life. Accordingly, three variations of the end weld configuration at the cover plate detail were investigated.

2.2 Experiment Design

Grade 345W Specimens - Eighteen W690x192 rolled wide flange beams with welded transverse stiffeners and cover plates were fatigue tested. The beams conformed to ASTM A 588 having minimum Fy = 366-435 MPa. The cover plates and stiffeners

were made from structural steel plates conforming to ASTM A 709 Grade 345W having minimum Fy = 407 MPa. Transverse stiffeners were provided over the full depth of the girder, welded to both the flanges and to the web. The weld details at the connections of transverse stiffener to the flange and web in flexural tension were considered critical for investigation. Cover plates were provided towards both ends of the girders. Details of the specimens are shown in Fig. 2. Three end weld configurations at cover plate were investigated. They were identified as: CP1 for cover plate detail having 13 mm end weld ($t_w = 0.5t_{cp}$; t_w: thickness of weld, t_{cp}: thickness of cover plate), CP2 for cover plate detail that did not have any end weld, and CP3 for cover plate detail with approximately 25 mm end weld ($t_w = t_{cp}$). Based on three different combinations of detail types CP1, CP2, and CP3 at the ends of a beam, the test specimens were grouped in three types. Type I specimens comprised detail CP1 at one end and detail CP3 on the other, type II specimens consisted of details CP1 and CP2, and type III specimens had detail CP3 at both ends. All welds were fillet welds and all the investigated details were treated by UIT.

A partial factorial experiment design was carried out at two S_{min} levels and at various S_r levels. This led to several R-values ranging between 0.05 and 0.55 depending on the combination of S_{min} and S_r. The test matrix is shown in Table 1. The specimens were distributed in eight cells in the factorial and the distribution was uneven. Originally the specimens were distributed evenly in six cells of three each (Roy, 2001). After a few initial tests of cover plate details CP1 and CP2, it was evident that further investigation of these detail types would not provide any gainful results. Accordingly, these details in the remaining specimens were modified to type CP3, the specimens were changed to type III,

and the test factorial was rearranged. The tests corresponding to the lowest three stress ranges at higher S_{min} were conducted to establish the fatigue limit for the CP3 details.

Grade HPS 690W Specimens - Eight built-up girders with welded stiffeners were fabricated from Grade HPS 690W having minimum F_y = 725-760 MPa. Six of these specimens were 10 mm x 762 mm deep with 25 mm x 178 mm wide flanges (Fig. 3). The other two specimens were 851 mm deep having 254 mm wide compression flange and 178 mm wide tension flange. Transverse stiffeners were provided over the full depth of the girder, welded to both the flanges and to the web.

Among all the fatigue tests that were conducted on the Grade HPS 485W and the Grade 345W specimens, only one stiffener detail developed fatigue crack from a weld fabrication defect at the toe. The primary objective of this phase of the experimental program was, therefore, to determine the enhancement in fatigue limit of the transverse stiffener-flange welds treated by UIT, and to establish the corresponding limiting value of R. Accordingly, a partial factorial experiment design was carried out at four S_r and five S_{min} levels, generating four different R-values of 0.32, 0.5, 0.56 and 0.6. The test matrix is shown in Table 2. The specimens that did not develop any detectable fatigue crack after being cycled beyond the 95% confidence limit to 95% failure life of longitudinal web-flange weld (Keating and Fisher, 1986), were re-tested at an elevated S_{min}. In Table 2, these specimens are indicated by an asterisk (*) suffixed to the specimen identifiers. It was assumed that the original combination of S_{min} and S_r was lower than the fatigue limit for the treated stiffener weld details and as such did not contribute to the fatigue damage

at the toe of the welds. Accordingly, the results from the re-tests are presented as additional data points in the S-N plots.

2.3 Treatment

The treatment was carried out according to the manufacturer's procedure document (Applied Ultrasonics, 2000). The operating frequency of the ultrasonic generator was 27000Hz. For normal conditions of application, the indenters consisted of four 3 mm diameter pins, fitted in a single holder. For weld toes situated in tight corners, a specially designed tapered holder consisting of only one 5 mm diameter pin was used. The treatment was carried out in short multiple passes. On average 3-5 passes at an average tool speed of 0.3m/min were made at a particular location to ensure a smooth uniform profile of the weld toe. Efforts were made to remove sharp transitions, re-entrant corners, and excessive convexity in weld toe profile. The intensity of the treatment was controlled by setting the level of output power range on control box. Proper operation of the equipment was ensured by the electronic display on the control box, which indicated the operating amplitude of the indenters, and was maintained at 30-35 μm. The adequacy of the treatment was ensured by adopting the operating procedures consistently and by visual inspection of the treated surface at 10X magnification. A well-treated toe manifested a shiny uniform groove free of any marks of original weld toe line. Signs of excessive cold working and plastic deformation with formation of metal flakes were evident.

2.4 Fatigue Tests

A schematic diagram of the test setup is shown in Fig. 4. The tests were conducted at constant amplitude fatigue loading in bending. The frequency of the tests ranged between 1 Hz and 4.3 Hz and the maximum jack capacities were 490 KN or 1335 KN depending on the applied maximum load. The tests were conducted either using AMSLER made variable stroke pulsators or VICKERS made computer controlled closed loop hydraulic system. All tests were load controlled and were monitored by strain gages mounted on the outer face of the tension flange. Stress ranges were controlled at the inner face of the tension flange for weld details at transverse stiffener, and at the outer face of the tension flange in case of the weld details at the cover plate. The data acquisition system comprised VISHAY switch and balance box, strain indicator and peak reader, or computerized DAYTRONIC signal conditioner and TESTPOINT application. The specimens were periodically inspected for fatigue cracks, visually with the aid of a magnifying glass. Tests were discontinued when a fatigue crack grew through the thickness of the flange into the web, and in most cases the tension flange completely fractured at the time of terminating the tests. In cases where the details did not develop any fatigue crack, the tests were discontinued after being cycled beyond the 95% confidence limit to 95% failure life of the least critical as-welded detail category in the specimen.

3. Fatigue Test Results

3.1 Failure Modes

Grade 345W specimens failed by fatigue fracture of the tension flange at the end of one of the cover plate details, except for G5, G11, G12 and G1-2. These type III

specimens did not develop any fatigue crack even after being subjected to $15x10^6$ stress cycles. All the five specimens containing both CP1 and CP3 type details developed fatigue cracks at detail CP1. These cracks initiated at the weld toe except for one case, where it started from a lack of fusion defect at the root. The details type CP2 developed fatigue cracks at the termination of the longitudinal weld. All the fractured CP3 type details developed fatigue cracks at the toe. No fatigue cracks were detected in any of the stiffener details when the tests were discontinued. During metallographic studies after completion of the tests, however, small fatigue cracks were detected in a couple of stiffener details that did not lead to fracture.

The Grade HPS 690 W specimens HPS2, HPS4, and HPS7 developed fatigue cracks from weld porosity at the root of the longitudinal web-flange weld. Specimen HPS1 developed fatigue crack originating from oxide inclusions at the surface of the flange plate. In specimen HPS8, fatigue crack developed from the remnant of a burn mark at the side of tension flange that was not completely ground out during fabrication. These specimens were all tested at $R \leq 0.5$. In specimens HPS3*, HPS5, and HPS6*, fatigue cracks developed at the transverse stiffener weld. These specimens were tested at R>0.5. Two of these cracks initiated from hot-cracking defects at the root and the other developed at the treated toe. Specimens HPS3 and HPS6 did not develop any detectable fatigue cracks when cycled at $R \leq 0.5$. These tests were discontinued after respectively $7.5x10^6$ and $20x10^6$ cycles.

3.2 S-N plots

Fatigue life versus the average recorded nominal stress range data for the treated cover plate and stiffener details are plotted on the current AASHTO specified S-N curve as shown in Figs. 5 and 6. These curves correspond to 95% confidence limit to 95% failure life of various as-welded detail categories (Keating and Fisher, 1986). Data points corresponding to the treated details that did not develop detectable fatigue cracks at the time of discontinuing the tests are indicated as "run-out". Test results demonstrate that all the details treated by UIT achieved substantial enhancement in fatigue strength. Figure 5 shows that all five CP1 details exceeded Category D resistance at low S_{min} corresponding to $R \leq 0.1$ and in particular, two of the details exceeded Category B resistance curve at a lower S_r. The CP3 details that were tested at lower S_{min} i.e., at $R \leq 0.1$ and at low S_r, did not develop any fatigue cracks. These "run-out" data suggest an elevation in fatigue limit exceeding that of Category B for this type of detail, treated by UIT. At higher R, the enhancement in fatigue strength for CP3 details reduced progressively; test data followed the slope of Category D resistance curve and the fatigue limit of the treated details exceeded that of Category C. Increase in fatigue life for CP2 details was limited to one category only.

Among all the test specimens, only four treated stiffener details developed fatigue cracks, one in HPS Grade 485W specimen, and three in Grade HPS 690W specimens. In Grade 345W specimens test data on stiffeners were limited by failure of cover plate details. The "run-out" data points in Fig. 6, corresponding to these specimens, indicate substantial increase in fatigue resistance of treated stiffener details. In Grade HPS 690W

specimens, the fatigue cracks developed only when tested at $R > 0.5$. Nevertheless, all the fatigue fracture data exceeded Category B fatigue resistance in the infinite life regime.

4. Discussion and Recommendations

From the test results it is evident that enhancement in fatigue resistance of the treated details was dependent on both S_r and S_{min}. Although substantial improvement was realized at the lower S_{min}, the beneficial effect of the treatment reduced when subjected to high S_{min} after treatment. This phenomenon is typical of any improvement technique that modifies residual stress through plastic deformation, and agrees with data from previous research. If applied S_{max} is sufficient to cause generalized yielding at the weld toe, the localized plasticity may erase a large portion of the beneficial compressive residual stress and the enhancement in fatigue life in that case will not be substantial. The extent of improvement is, therefore, dependent on the stress history at the weld toe i.e., on the sequence of application of the treatment and the applied stresses, both permanent and cyclic. Evidently, the magnitude of the actual stress ratio R must be evaluated with respect to the applied stresses after application of the post-weld treatment. At high values of S_{min}, substantial enhancement may be achieved when the surface treatment is applied under gravity load as was reported by Fisher et al. (1979) for weld toe treated by air hammer peening.

In general, fatigue crack at the treated cover plate welds originated at the weld toe. In high fatigue life regime and particularly for smaller weld size, however, this failure mode may change to fatigue crack growth from weld root in the presence of a large weld discontinuity. This was evident from fatigue performance of the CP1 details.

For optimum performance of UIT, it is desirable to match the fatigue crack growth life from root defects to that from the treated toe, where the beneficial effect of treatment delays or prevents the crack initiation and growth. For the CP3 details this was achieved by increasing the size of the end weld at cover plate to the plate thickness, which reduced stress concentration at the root and therefore maximized the beneficial effect of the treatment. Therefore, sufficient weld size must be provided in design for optimizing the performance of all treated welded details.

Design recommendation for enhancement in fatigue strength of welded details treated by UIT is indicated in Figs. 5 and 6 by the dashed lines. In case of CP3 cover plate details, having leg size of end weld equal to the thickness of the plate, for $R \leq 0.1$ the fatigue strength may be increased to AASHTO Category B in the infinite life region and to AASHTO Category D in the finite life regime. For $0.1 < R \leq 0.5$, the fatigue resistance may be increased to AASHTO Categories C and E respectively, for infinite and finite life regions. In case of CP1 cover plate details, with end weld size equal to half the thickness of the plate, the fatigue strength may be increased to AASHTO Category B in the infinite life region and to Category D in the finite life regime, only for $R \leq 0.1$. This scenario is applicable for most of the existing cover plate end welds in service, where fatigue life may be enhanced by UIT provided it may be ensured by non-destructive evaluation prior to application of treatment that no fatigue crack has initiated at the weld toe. To avoid fatigue fracture due to cracks developing from root, however, these details should be inspected periodically according to the inspection procedure for as-welded details. Fatigue strength of stiffener details may be increased to Category B in the infinite life region, but no improvement is recommended in the finite life region because of lack

of sufficient data. Also, in view of available experimental data the improvement is limited to a maximum R of 0.5. In any event, the maximum improvement that can be achieved will be bound by Category B design curve corresponding to fatigue fracture limit state of longitudinal web-flange weld, due to fatigue crack growth from root defects.

5. Effects of UIT

5.1 Changes in Geometry and Microstructure

After fatigue tests several weld details and crack surfaces were cut out from the specimens and were examined for origins of fatigue cracks. Figure 7 shows a photomicrograph of a typically treated weld toe at 100X magnification. It is evident that UIT severely deforms the metal in the vicinity of the treatment. The extent of treatment and the severity of plastic deformation are visible from the change in microstructure in the base metal near the treated weld toe. The grain shapes have become progressively less elongated with depth below the surface and also along the surface away from the treated area. At the treated surface, individual grains could be barely distinguished. Figure 8 shows a typical exposed crack surface that originated from the toe of a cover plate detail. The crack surface indicates a classical two stage crack growth pattern with cracks initiating at multiple locations along the weld toe and coalescing to form a long shallow crack before growing as semi-elliptical surface crack until penetration of the flange. Figue 9 shows approximately 20X and 109X magnification of the toe by a scanning electron microscope (SEM). The depth of plastic deformation due to UIT is manifested by the dense laminar structure extending up to about 0.2 mm from the surface. Any microscopic discontinuities inherent to the welding process could not be identified at the weld toe. Radaj and Sonsino (1998) have reported studies conducted by various

researchers that indicated initial crack-like micro discontinuities at welded joints varying between 0.01 and 0.4 mm. A more recent study conducted by Reynolds (1993) concluded that for Submerged Arc Welding (SAW) process the discontinuities at weld toe due to slag inclusion, micro cracking and gas pores were much less than 0.1 mm. It therefore appears that UIT blunted any initial discontinuities at the weld toe due to welding and deterred the development of fatigue cracks at the treated toe.

Metallographic studies of several treated weld toes revealed lap type defects as shown in Fig. 10. These defects resulted from extensive surface cold working by UIT. Although these defects were mostly parallel to the surface, in some cases they turned into the weld metal/HAZ. An approximate measurement of these lap defects indicated that they were about 0.25 mm deep, which is in the order of crack-like discontinuities at an as-welded toe. It may be possible that these crack-like lap defects grew under favorable stress conditions eventually leading to fatigue fracture of some of the treated details. Fisher et al. (1979) also made similar observations for weld toes treated by air hammer peening.

As seen in Fig. 7, UIT modified the as-welded toe geometry by introducing an undercut. The changes were assessed by measuring the width, depth and radius of curvature of the undercut in photomicrographs of several treated weld toes at 100X magnification. Approximate lower bound values of these measurements are shown in the figure.

5.2 Changes in Residual Stress Field

Changes in residual stress distribution adjacent to the fillet weld toes before and after application of UIT were reported by Trufyakov et al. (1995) and Janosch et al. (1995). These measurements were made by hole-drilling method up to 0.9 mm depth. Another measurement of residual stresses in ultrasonic impact treated welded joints by layer removal was also reported by Trufyakov et al. (1995). Spatial distribution of residual stresses adjacent to a weld toe in a simulated cover plate detail similar to the test specimen described earlier, was measured by Neutron Diffraction technique before and after application of UIT (Prask et al., 2001). Similar measurements in ultrasonic impact treated base metals were also reported by Prask et al. (2002), and Cheng et al. (2003). All these measurements indicate that approximately same level of compressive residual stresses as the yield stress of the base metal was introduced in the surface layer following the treatment.

6. Estimation of Fatigue Strength

6.1 Theoretical Background

Fatigue strength for infinite life of an ultrasonic impact treated end weld in a cover plate was estimated using a stress-life approach. As was revealed by metallographic studies, the localized plastic deformation associated with post-weld treatment blunted the crack like micro discontinuities in the as-welded toe, and introduced a well defined undercut. Thus, the performance of a treated detail may be modeled as that of a notch with finite radius, where initiation of fatigue crack dominates the total fatigue life. Determination of fatigue strength in the infinite life regime under constant amplitude loading requires that fatigue fracture be avoided independent of

service life. The stress and strain at the notch root must be predominantly elastic in that condition to suppress cyclic crack initiation or, at the least crack propagation. Then, following a simplified approach (Fuchs and Stephens, 1980) an approximate lower bound estimate of fatigue strength can be made based on the long life alternating (R = -1) fatigue limit or the endurance limit (S_f) of an un-notched specimen, modified by the mean stress effect and the fatigue notch factor (K_f) of the detail. The fatigue notch factor relates the un-notched fatigue strength of a member to its notched fatigue strength at a given life.

Smith et al. (1970) suggested the following stress-strain function governing fatigue to include the effect of mean stress,

$$\sqrt{(\sigma_{\max} \varepsilon_a E)} \quad = \quad C \tag{1}$$

where, σ_{max} is the maximum stress, ε_a is the strain amplitude, E is modulus of elasticity, and C is a material constant. As long as the stresses and strains remain elastic, substituting $\sigma_{max} = \sigma_0 + \sigma_a$, where σ_0 is the mean stress, and σ_a is the stress amplitude, the equation can be re-written as,

$$(\sigma_a + \sigma_0)\sigma_a \quad = \quad C^2 \tag{2}$$

For a smooth specimen subjected to zero mean stress, the material constant C must be half the alternating fatigue limit, or the endurance limit S_f at a given life.

Now, consider the treated weld toe idealized as a notch and subjected to nominal stresses S_{min} and S_{max}. Then,

$$S_r = S_{\max} - S_{\min} = S_{\max}(1-R) = 2S_a$$
$$S_m = \frac{1}{2}(S_{\max} + S_{\min}) = \frac{S_r}{2}\frac{(1+R)}{(1-R)} \tag{3}$$
$$R = \frac{S_{\min}}{S_{msx}}$$

where, S_r is the nominal stress range, S_a is the nominal stress amplitude, and S_m is the nominal mean stress. Considering the effect of residual stress field introduced at the treated surface, σ_R, as a mean stress effect, and substituting for σ_a and σ_0 at the notch root in Eq.2, obtain,

$$\sigma_a = K_f \frac{S_r}{2}; \quad \sigma_0 = K_f S_m + \sigma_R$$
$$\frac{K_f{}^2}{(1-R)} S_r{}^2 + \sigma_R K_f S_r = \frac{S_f{}^2}{2} \tag{4}$$

and,

$$S_r = \frac{1-R}{2K_f}\left[-\sigma_R + \sqrt{\sigma_R{}^2 + \frac{2}{1-R} S_f{}^2}\right] \tag{5}$$

Eq.5 provides a relationship between allowable S_r and R for a particular notch geometry and material. In case of a compressive residual stress equal to the yield stress, this equation is valid only for $0 \leq R \leq 1$, so that elastic condition is maintained at the notch root. The fatigue notch factor may be obtained from the theoretical stress concentration factor, K_t, at the notch root, using the empirical relationship proposed by Peterson (1959),

$$K_f = 1 + \frac{K_t - 1}{\left(1 + \frac{a}{r}\right)} \quad (6)$$

where, r is the notch root radius, and a is a material parameter. For normal steels, Lawrence et al. (1978) recommended that a rough estimate of a (in mm) be obtained from the ultimate tensile strength, S_u (in MPa) of the material as,

$$a = 2.5 \times 10^{-5} \left[\frac{2068}{S_u}\right]^{1.8} \quad (7)$$

6.2 Determination of Stress Concentration Factor

The theoretical elastic stress concentration factor K_t for the treated weld toe geometry was determined numerically using submodel analysis technique in commercially available finite element code ABAQUS (2003). The analysis was carried out in three levels. In the first level a symmetric half model of the Grade 345W beam specimen was analyzed. This model contained all the stiffeners and cover plates as the test specimen, but excluded the actual weld notches. In the second level a submodel of the cover plate end detail was analyzed, where the weld was modeled as a notch having 135^0 flank angle with a theoretically zero toe radius. Finally, a submodel of a very small region at the weld toe was analyzed. An idealized undercut about 0.4 mm deep and having a root radius of 3 mm was introduced at the weld toe to simulate the geometric effect of the treatment. The value of the root radius was chosen based on the measurements made during metallographic studies reported earlier. The submodel of the treated weld toe is shown in Fig. 11. Twenty node quadratic reduced integration

hexahedral elements were used for all analyses. The smallest dimension of element at the notch root was of the order of 0.075 mm.

The global model was analyzed for an actuator force of 445 KN (100 kips) accordingly to the loading scheme shown in Fig. 4. The submodels were driven by displacement boundary conditions. The maximum principal stress versus distance along a longitudinal section through the cover plate is plotted in Fig. 12. The nominal principal stress at the weld toe is extrapolated linearly from the variation of stresses away from the influence of the weld notch. The theoretical elastic K_t for the treated weld toe was determined as 4.34.

6.3 Fatigue Limits

The average ultimate strength of the Grade 345W beam specimens from different heats was determined to be 515 MPa from the mill report. Using this value for S_u in Eq.7, and using the Peterson's equation along with the theoretical K_t determined from the Finite Element Analysis, the fatigue notch factor was obtained as 4.0. From the same mill report, the average yield strength of the specimens was determined as 386 MPa. It was assumed that a compressive residual stress of 386 MPa was introduced in the surface layer of the weld toe treated by UIT.

Fatigue limit of steel alloys usually vary between 0.35 and 0.6 times the tensile strength of the material, and often is estimated to be one-half the tensile strength for low and medium strength steel having $S_u \leq 1400$ MPa (Fuchs and Stephens, 1980). Most of these data are based on fully reversed uniaxial fatigue tests of small highly polished un-notched specimens and 10^6 to $5\text{x}10^8$ cycles to failure. The condition at the treated weld

toe is, however, different from the above conditions. The treatment introduces perceptible roughness at the weld surface, which is expected to reduce the fatigue strength. On the other hand, UIT increases the hardness of the treated surface through work hardening. This is expected to increase the fatigue strength since a direct relationship exists between the tensile strength and hence the fatigue strength of a material, and its hardness. Moreover, the treated weld toe consists of a heterogeneous microstructure involving the weld metal, the base metal, and the heat affected zone (HAZ), where the fatigue strength is generally unknown. Therefore, as an approximation, the endurance limit of the treated weld toe has been assumed as half the tensile strength of the base material. For Grade 345W specimens, this yields alternating fatigue strength of 257.5 MPa, which was rounded down to 250 MPa. It should, however, be noted that in absence of sufficient test data the above value of fatigue strength is merely an approximation, and has been chosen to obtain an estimate of the fatigue limit of the cover plate end weld details treated by UIT.

Using $K_f = 4.0$, $\sigma_R = -386$ MPa, and $S_f = 250$ MPa in Eq. 5, the allowable stress ranges for the cover plate details for R = 0.5 and R = 0.1 were obtained respectively as 64 MPa and 104 MPa. These values are quite close to the constant amplitude fatigue limit for the as-welded AASHTO Category C and Category B details which are specified respectively as 70 MPa and 110 MPa. Thus, the analysis justified the model used for estimation of the fatigue strength of the ultrasonic impact treated cover plate details and substantiated the suggested fatigue limits that were proposed based on fatigue test data.

7. Conclusions

1. The UIT technique is a feasible alternative to conventional post-weld treatment techniques such as air hammer peening or gas tungsten arc re-melting. It was found to substantially enhance the fatigue life of treated transverse weld at cover plate and stiffeners.

2. Cover plate end welds having weld size equal to the thickness of the cover plate performed better than the other type of cover plate details. In particular, this type of detail optimized the enhancement in fatigue strength of the treated details. It is recommended to suitably increase the size of all welds enhanced by UIT in new construction, to suppress fatigue crack growth from root defects and to optimize their performance.

3. Enhancement in fatigue life for cover plate with no end weld is limited to one design category and it is recommended that this detail type not be used.

4. UIT improved the weld toe geometry and reduced the micro discontinuities at the weld toe through surface erosion, plastic deformation, and change in microstructure. It also introduced beneficial compressive residual stress to the order of yield stress of the material at the treated surface. Cumulatively these improvements enhanced fatigue strength of the treated details by increasing the fatigue crack initiation life and the fatigue crack growth threshold.

5. The enhancement in fatigue strength was dependent on the stress ratio R. It was more pronounced at low R, and particularly at lower S_{min} and at lower S_r.

6. Fatigue strength of as-welded Categories C′ (transverse stiffener) and E′ (cover plate end) weld details may be enhanced by UIT according to Table 3.

7. Estimated fatigue strength of treated cover plate details, based on a simplified stress-life approach, substantiated the recommended values of fatigue limits for R = 0.1 and 0.5.

Acknowledgements

This study was conducted at the Department of Civil and Environmental Engineering and at the ATLSS Engineering Research Center of Lehigh University, Bethlehem, PA, USA. The work was partially supported by the Federal Highway Administration (FHWA), the Pennsylvania Infrastructure Technology Alliance (PITA), and, the American Iron and Steel Institute (AISI). Special acknowledgement is due to Applied Ultrasonics, Birmingham, AL, USA for supplying the UIT equipment and particularly to Dr. Efim Statnikov for providing application guidance. The authors will also like to thank Dr. Ben Yen, Dr. Eric Kaufmann and the support staff of the Fritz Lab and the ATLSS Center for their valuable contribution to the project.

References

ABAQUS Inc. (2003). *ABAQUS analysis user's manual*. version 6.4, ABAQUS, Inc., Pawtucket, RI, USA.

American Association of State Highway and Transportation Officials. (2003). *AASHTO LRFD Bridge Design Specifications – U.S. Units*. 2003 Interim Revisions, American Association of State Highway and Transportation Officials, Washington, D.C., USA.

Applied Ultrasonics. (2000). "Esonix Ultrasonic Impact Treatment: Technical Procedure Document." Applied Ultrasonics, Birmingham, AL, USA.

Booth, G.S. (1981). "The fatigue life of ground or peened fillet welded steel joints - the effect of mean stress". *Metal Construction*, 13(2), p. 112-115.

Cheng, X., Fisher, J.W., Prask, H.J., Gnäupel-Herold, T., Yen B.T., and Roy, S. (2003). "Residual stress modification by post-weld treatment and its beneficial effect on fatigue strength of welded structures." *International Journal of Fatigue,* Elsevier, 25(9-11), p. 1259–1269.

Fisher, J.W., Frank, K.H., Hirt, M.A., and McNamee, B.M. (1970). *Effect of weldments on the fatigue strength of steel beams, NCHRP, Report 102*, Highway Research Board, Washington, D.C., USA.

Fisher, J.W., Albrecht, P.A., Yen, B.T., Klingerman, D.J., and McNamee, B.M. (1974). *Fatigue strength of steel beams with transverse stiffeners and attachment,. NCHRP, Report 147*, Highway Research Board, Washington, D.C., USA.

Fisher, J.W., Hausammann, H., Sullivan, M.D., and Pense, A.W. (1979). *Detection and repair of fatigue damage in welded highway bridges. NCHRP Report 206*, Transportation Research Board, Washington, D.C., USA.

Fuchs, H.O., and Stepehens, R.I. (1980). *Metal fatigue in engineering*. John Wiley & Sons, New York, N.Y., USA.

Gross, J.H., and Stout, R.D. (2001). "Proposed specification for an HPS 100W Cu-Ni age-hardening ASTM A709 grade bridge steel." ATLSS Report No. 01-15, Center for Engineering Research on Advanced Technology for Large Structural Systems (ATLSS), Lehigh University, Bethlehem, PA, USA.

Gurney, T.R. (1979). *Fatigue of welded structures*. 2nd ed., Cambridge University Press, Cambridge, UK.

Haagensen, P.J, Statnikov, E.S., and Lopez-Martinez, L. (1998). *Introductory fatigue tests on welded joint in high strength steel and aluminum improved by various methods including ultrasonic impact treatment (UIT)*, *IIW, Doc. XIII-1748-98*, International Institute of Welding, Paris, France.

Janosch, J.J., Koneczny, H., Debiez, S., Statnikov, E.C., Troufiakov, V.J., and Mikhee, P.P. (1995). *Improvement of fatigue strength in welded joint (in HSS and in aluminum alloy) by ultrasonic hammer peening, IIW, Doc. XIII-1594-95*, International Institute of Welding, Paris, France.

Keating, P., and Fisher, J.W. (1986). *Evaluation of fatigue tests and design criteria on welded details*, *NCHRP, Report 286*, Transportation Research Board, Washington, D.C., USA.

Lawrence, F.V., Mattox, R.J., Higashida, Y., and Burk, J.D. (1978). "Estimating the fatigue crack initiation life of weld." *Fatigue Testing of Weldments, ASTM, STP 648*, D.W. Hoeppner, Ed., American Society of Testing and Materials, Philadelphia, PA, USA, p. 134-158.

Maddox, S.J. (1991). *Fatigue strength of welded structures*.2nd ed., Abington Publishing, Cambridge, UK.

Peterson, S.E. (1959). "Notch Sensitivity." *Metal Fatigue*, University of California Engineering Extension Series, George Sines and J.L. Waisman, Ed., McGraw-Hill Book Co., Inc., New York, N.Y., USA.

Prask, H.J., Gnaupel-Herold, T., Fisher, J.W., and Cheng, X. (2001). "Residual stress modification by means of ultrasonic impact treatment." *Proc. Annual Conference on Experimental and Applied Mechanics*, Society for Experimental Mechanics, Portland, OR, USA, p. 551-554.

Prask, H.J., Gnaupel-Herold, T., Luzin, V., Fisher, J.W., Cheng, X., and Roy, S. (2002). "Residual stress modification and fatigue life enhancement." *Trends in Welding Research: Proc. 6th International Conference*, ASM International, Phoenix, AZ, USA, p. 897-901.

Radaj, D., and Sonsino, C.M. (1998). *Fatigue assessment of welded joints by local approaches*. Abington Publishing, Cambridge, UK.

Reynolds, J.P. (1993). "The effect of welding process on the occurrence of weld toe microdiscontinuities in HSLA 80 steel." Masters Thesis, Dept. of Material Science and Engineering, Lehigh University, Bethlehem, PA, USA.

Roy, S. (2001). "Post-weld Enhancement of Welded Stiffeners and Cover Plates using Ultrasonic Impact Treatment." Masters Thesis, Dept. of Civil and Environmental Engineering, Lehigh University, Bethlehem, PA, USA.

Smith, I.F.C. and Hirt, M.A. (1985). "A review of fatigue strength improvement methods." *Canadian Journal of Civil Engineering*, 12, p. 166-183.

Smith, K.N., Watson, P., and Topper, T.H. (1970). "A stress-strain function for the fatigue of metals." *Journal of Materials*, JMSLA, 5(4), p. 767-778.

Statnikov, E.Sh. (1997a). *Applications of operational ultrasonic impact treatment (UIT) technologies in production of welded joints, IIW, Doc. XIII-1667-97*, International Institute of Welding, Paris, France.

Statnikov, E.Sh. (1997b). *Comparison of post-weld deformation methods for increase in fatigue strength of welded joints, IIW, Doc. XIII-1668-97*, International Institute of Welding, Paris, France.

Statnikov, E.S. (1999). *Guide for application of ultrasonic impact treatment for improving fatigue life of welded structures, IIW, Doc. XIII-1668-97*, International Institute of Welding, Paris, France.

Takamori, H. (1999). "Improving Fatigue Strength of Welded Joints." PhD dissertation, Dept. of Civil and Environmental Engineering, Lehigh University, Bethlehem, PA, USA.

Takamori, H., and Fisher, J.W. (2000). "Tests of large girders treated to enhance fatigue strength." *Transportation Research Record, 1696*, Transportation Research Board, 1, p. 93-99.

Trufyakov, V.I., Mikheev, P.P., Kudryavtsev, Yu. F., and Statnikov, E.S. (1995). *Ultrasonic impact treatment of welded joints, IIW, Doc. XIII-1609-95*, International Institute of Welding, Paris, France.

Wright, W. (1996). "Post-weld Treatment of A Welded Bridge Girder by Ultrasonic Hammer Peening." Internal Research Report, Federal Highway Administration, Turner Fairbank Highway Research Center, McLean, VA, USA.

Table 1. Test Matrix for Grade 345W Specimens

S_{min} (MPa)	S_r (MPa)						
	Cover plate details						
	52	62	67	72	97	124	152
10	…	…	…	…	G1(I)[a] G2(I) G3(I) G1-2(III) (R=0.09)	…	G7(I) G8(I) G9(III) G18(III) (R=0.06)
62	G11(III) (R=0.55)	G5(III) (R=0.5)	G10(III) (R=0.48)	G6(III) G12(III) (R=0.46)	G4(III) G13(II) G14(II) G15(III) (R=0.39)	G16(III) G17(III) (R=0.33)	…
	Stiffener details						
	69 (10)	83 (12)	90 (13)	97 (14)	131 (19)	166 (24)	200 (29)
14	…	…	…	…	G1(I) G2(I) G3(I) G1-2(III) (R=0.09)	…	G7(I) G8(I) G9(III) G18(III) (R=0.06)
83	G11(III) (R=0.55)	G5(III) (R=0.5)	G10(III) (R=0.48)	G6(III) G12(III) (R=0.46)	G4(III) G13(II) G14(II) G15(III) (R=0.39)	G16(III) G17(III) (R=0.33)	…

[a] "G" indicates "Girder; Arabic numerals indicate serial number of specimen and Roman numerals indicate

the specimen type.

Table 2. Test Matrix for Grade HPS 690W Specimens

S_{min} (MPa)	S_r (MPa) 97	110	131	138
63	…	…	HPS1 HPS2 HPS3 (R=0.32)	…
97	HPS6 (R=0.55)	…	…	…
110	…	HPS7 HPS8 (R=0.5)	…	…
138	…	HPS5 HPS6* (R=0.56)	…	HPS4 (R=0.5)
166	…	HPS3* (R=0.6)	…	…

Table 3 - Design Recommendations for UIT Details

As-welded Detail Category	Stress Ratio, R	Enhanced Detail Category: Finite Life	Enhanced Detail Category: Infinite Life
E′ ($0.5t_{cp} \le t_w \le t_{cp}$)	$R \le 0.1$	D	B
E′ ($t_w = t_{cp}$)	$0.1 < R \le 0.5$	E	C
C′	$R \le 0.5$	C′	B

Fig. 1. UIT Tool and Control Box

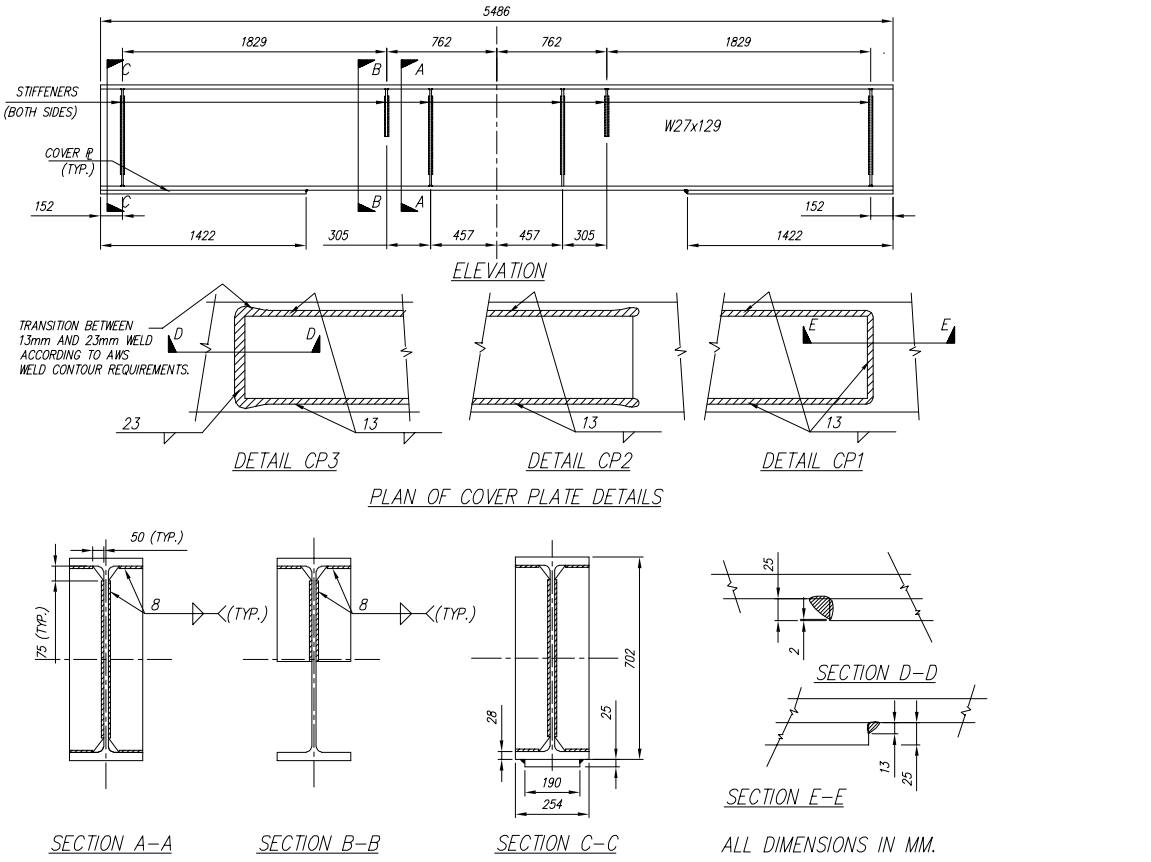

Fig. 2. Details of Grade 345W Specimens

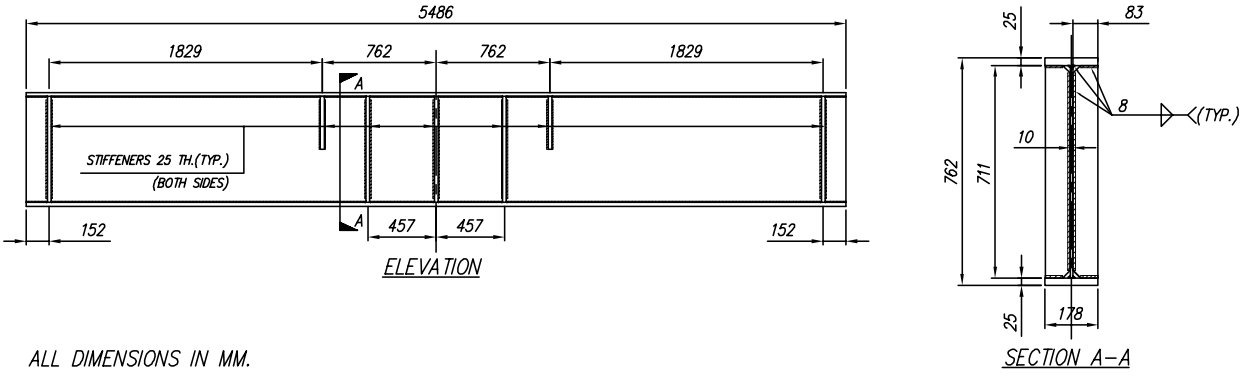

Fig. 3. Details of Grade HPS 690W Specimens

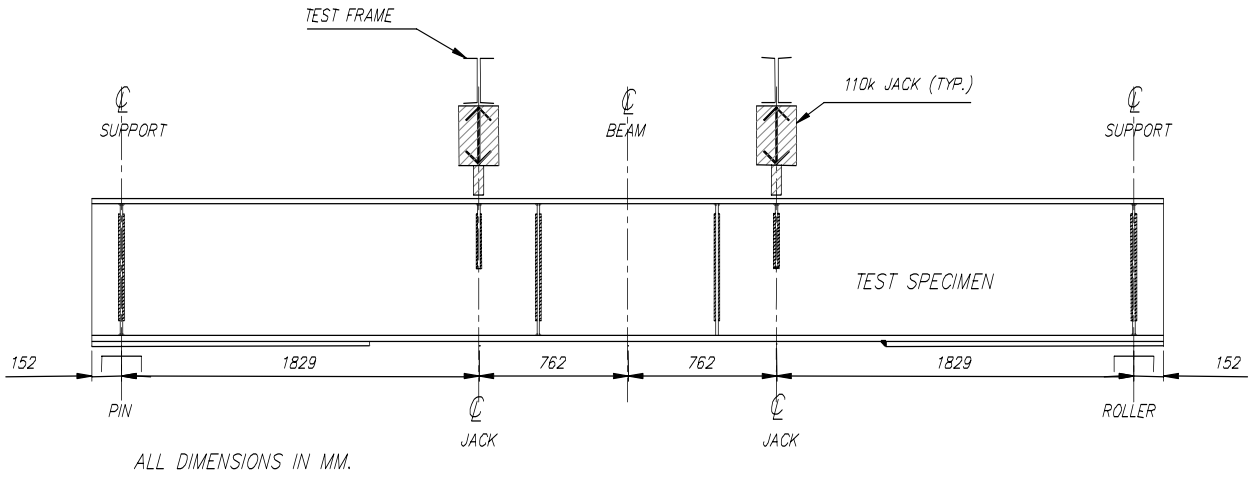

Fig. 4. Schematics of Test Setup

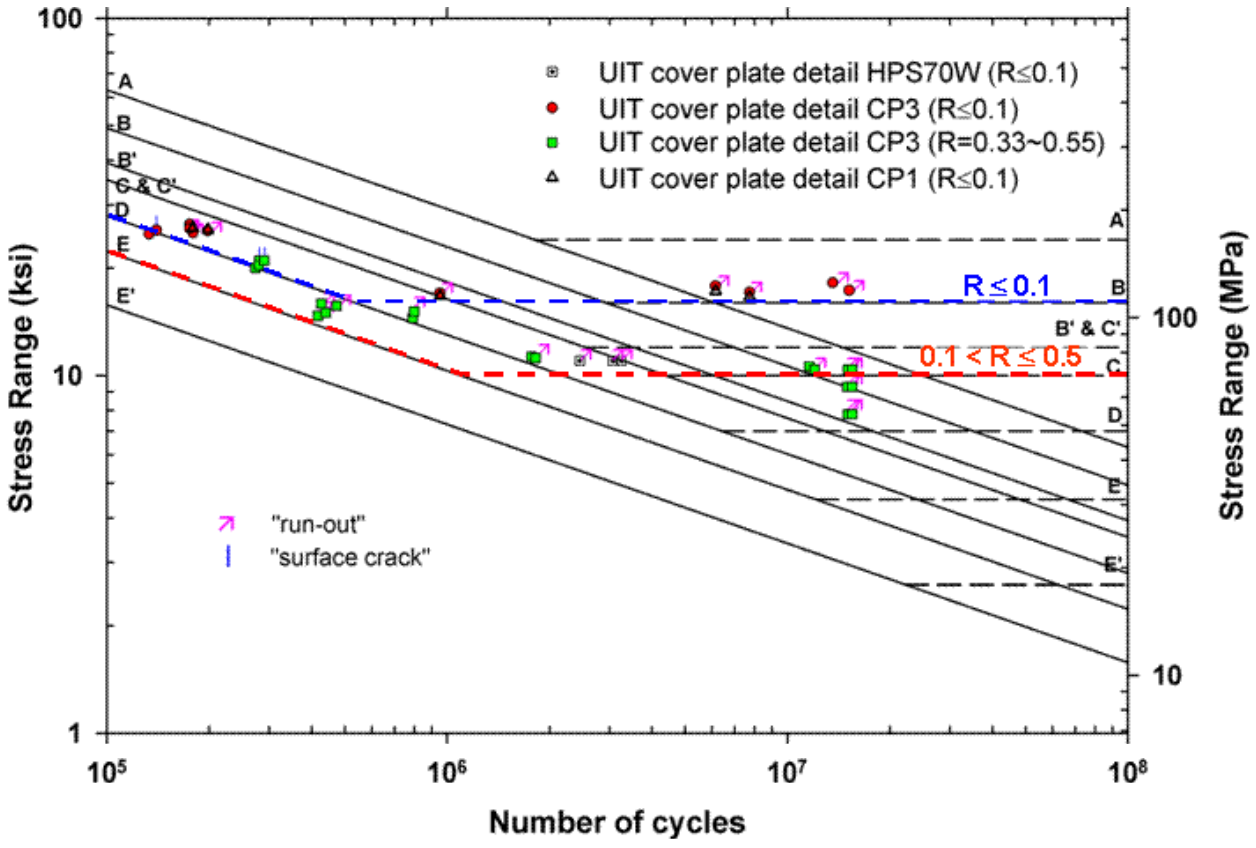

Fig. 5. S-N Curve for Cover Plate Details

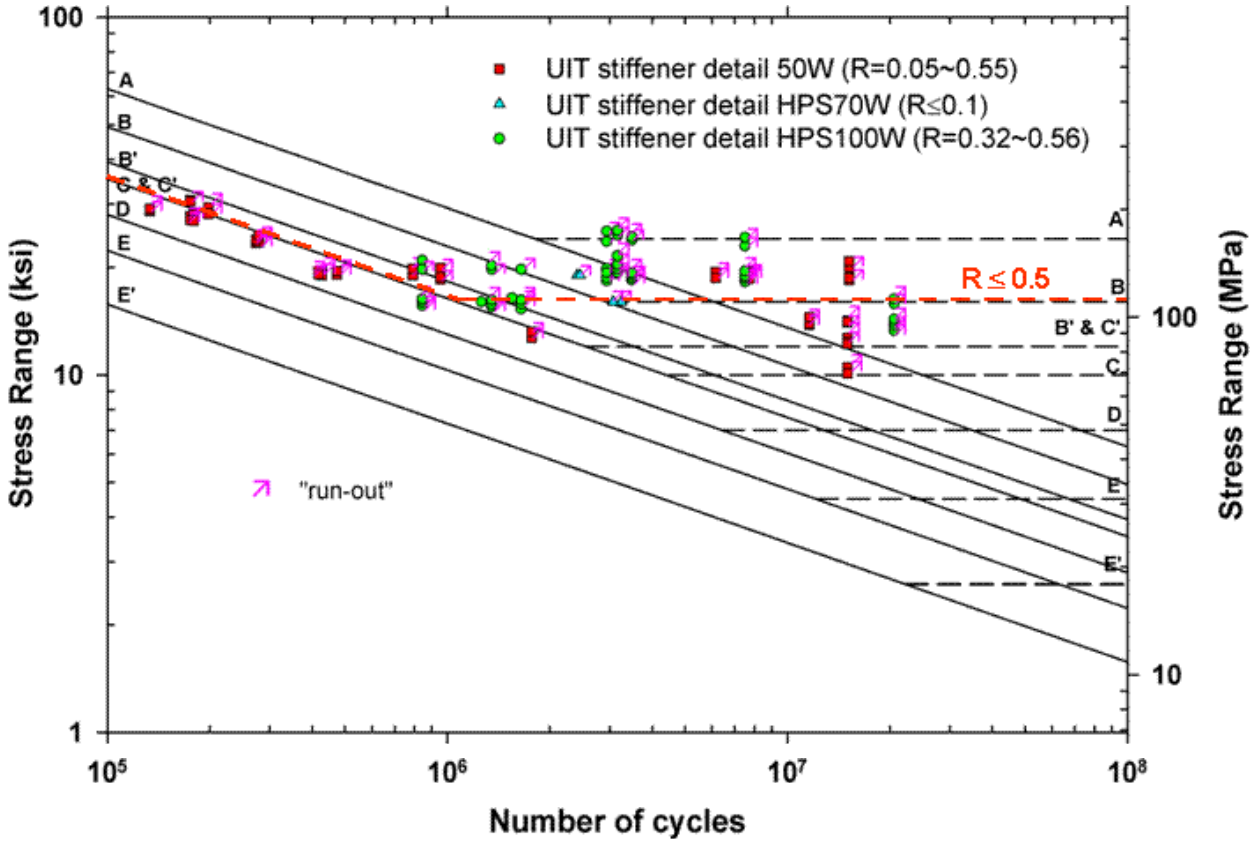

Fig. 6. S-N Curve for Stiffener Details

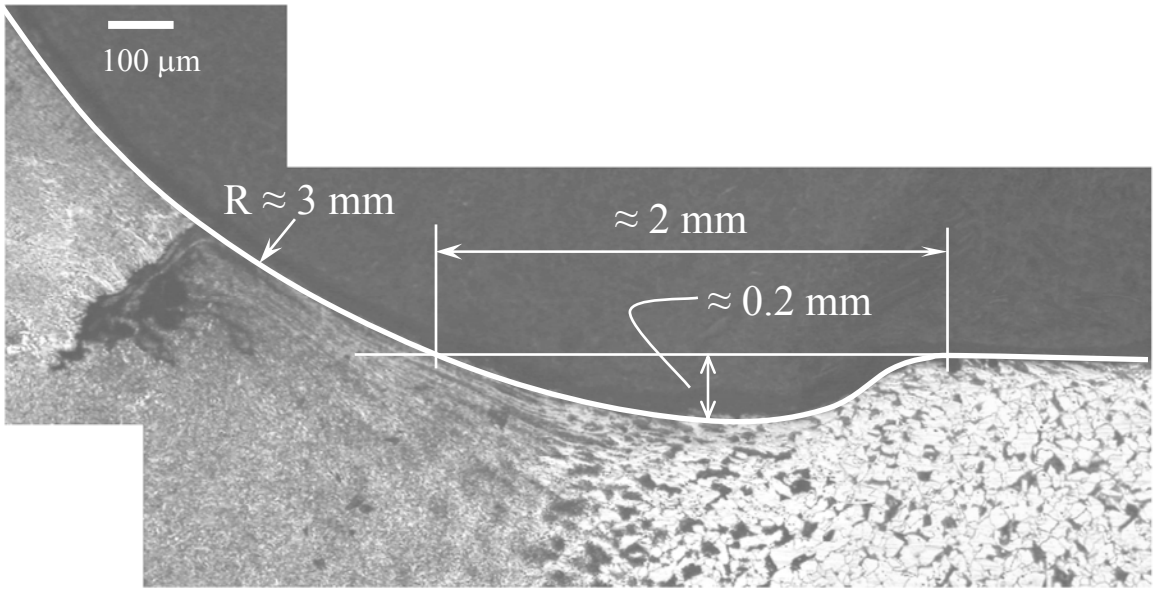

Fig. 7. Photomicrograph at 100X

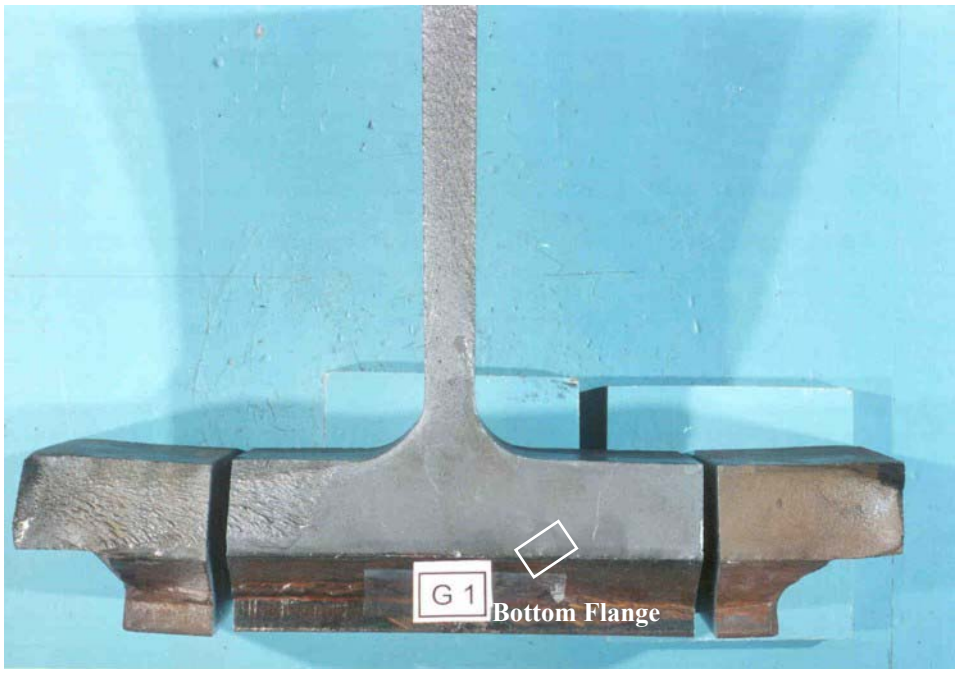

Fig. 8. Exposed Crack Surface at Toe of Cover Plate End Weld

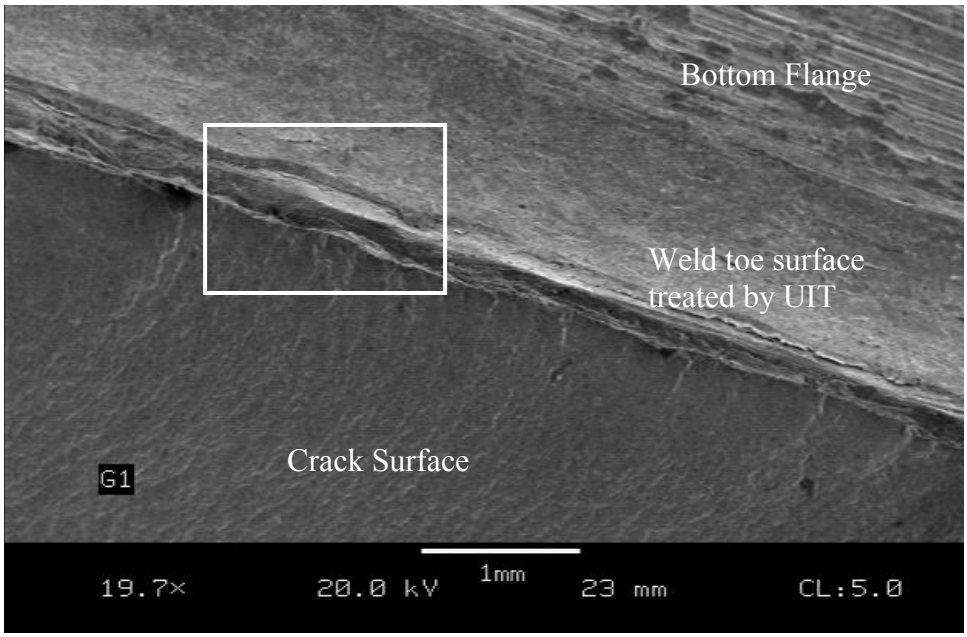

(a)

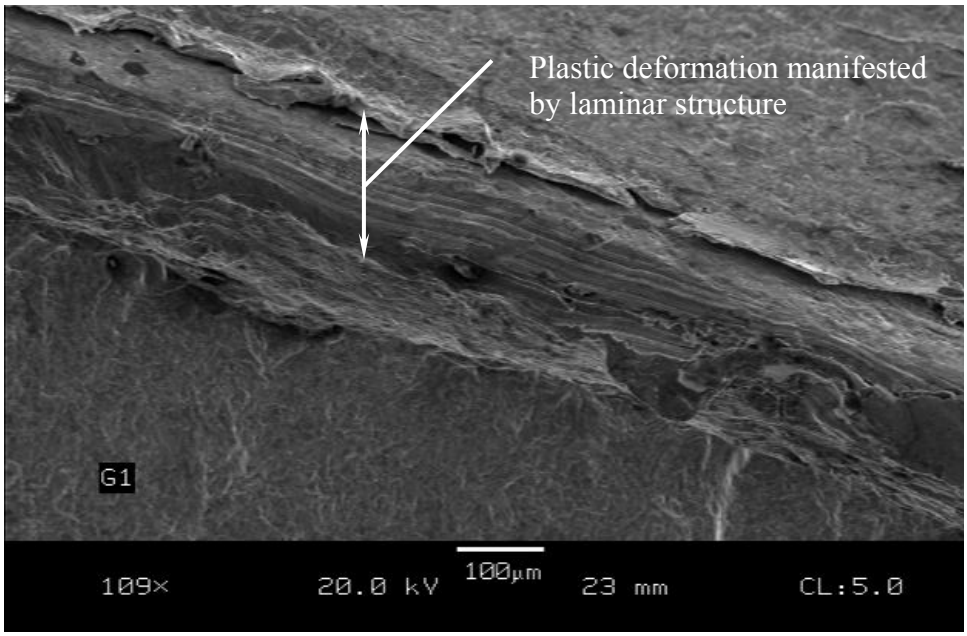

(b)

Fig. 9. Scanning Electron Microscopy at Crack Surface

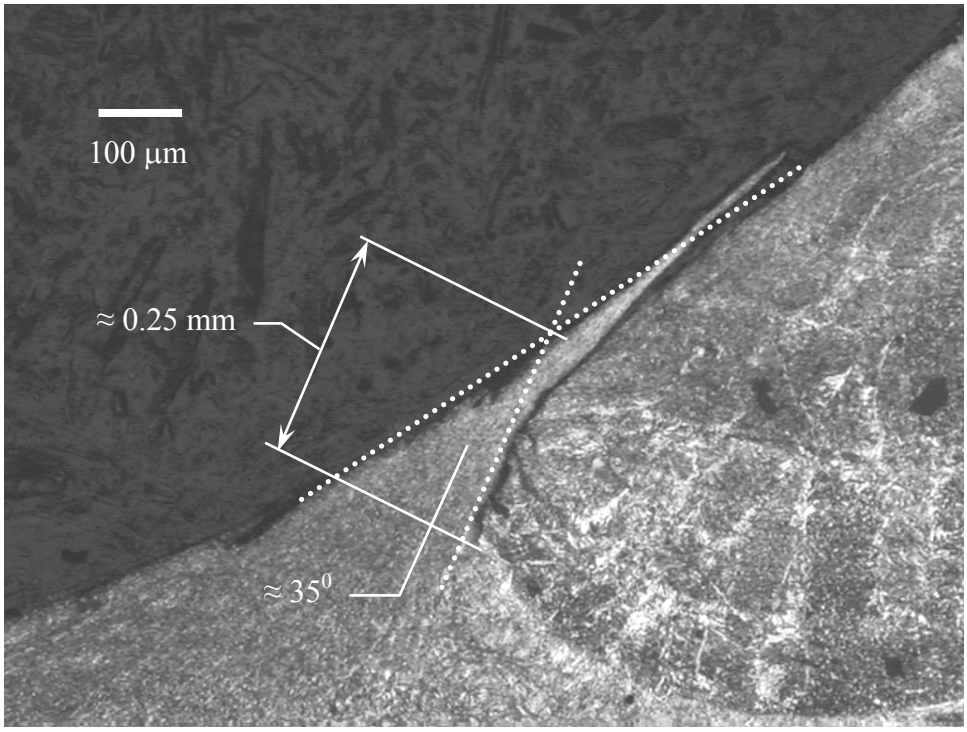

Fig. 10. Lap Type Defect

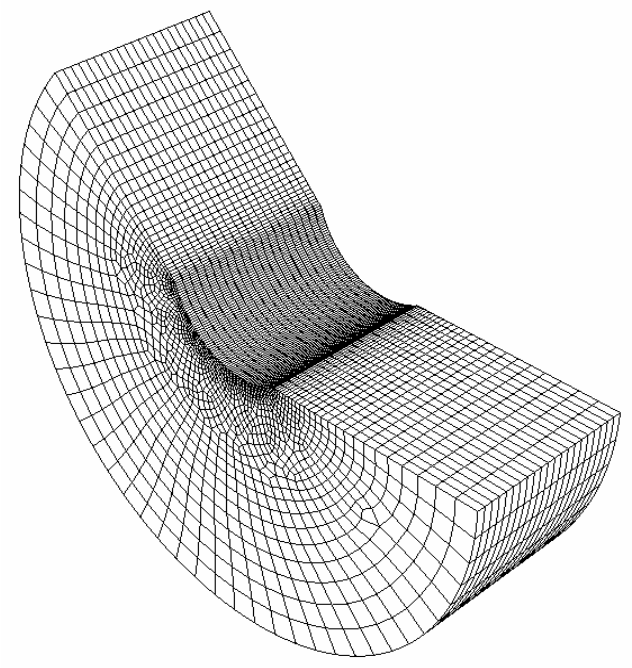

Fig. 11. Sub model of weld toe

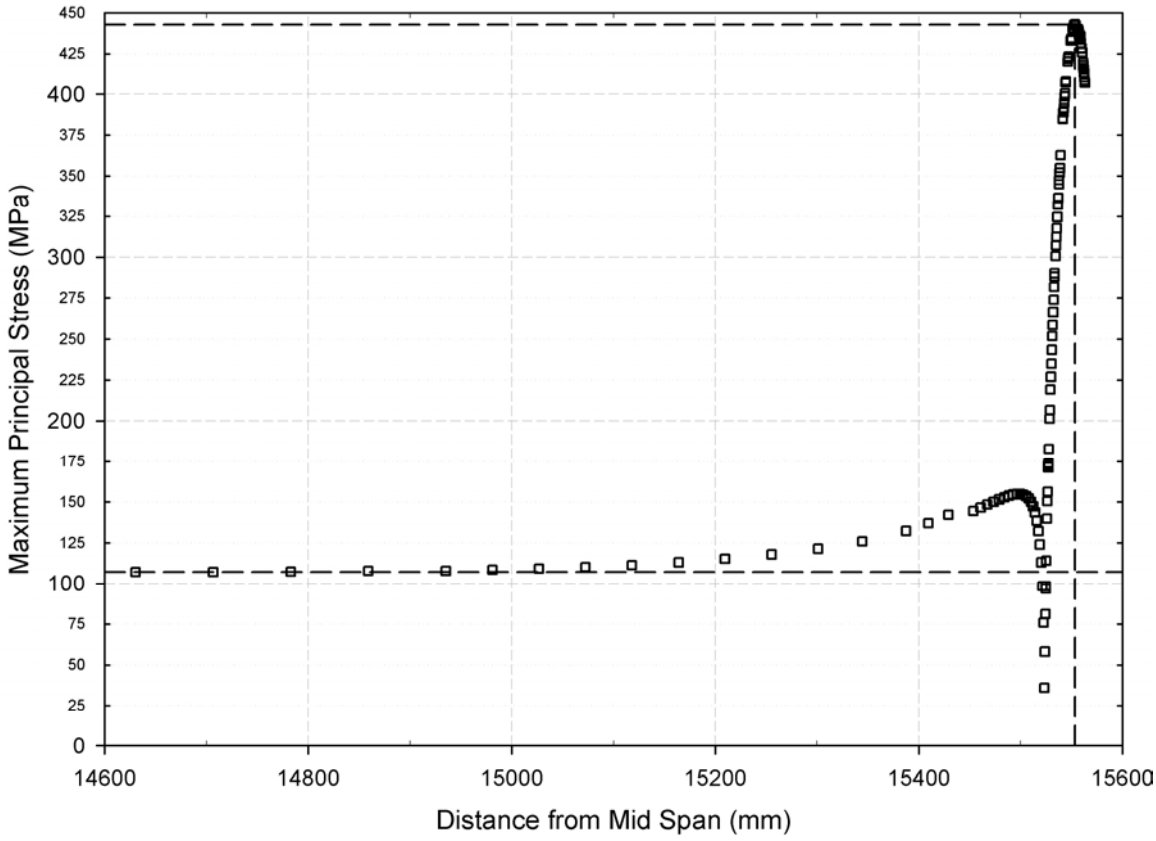

Fig. 12. Principal Stresses along Section Through Cover Plate